Investigation into the Settlement of a Case Study Building on Liquefiable Soil in Adapazari, Turkey

J. Quintero[1]; S. Saldanha[2]; M. Millen[3]; A. Viana da Fonseca[4]; S. Sargin[5]; S. Oztoprak[6]; and M. K. Kelesoglu[7]

[1]CONSTRUCT-GEO, Faculty of Engineering of Univ. of Porto, Rua Dr. Roberto Frias, s/n 4200-465 Porto, Portugal. E-mail: julieth@fe.up.pt
[2]CONSTRUCT-GEO, Faculty of Engineering of Univ. of Porto, Rua Dr. Roberto Frias, s/n 4200-465 Porto, Portugal. E-mail: asaldanha@fe.up.pt
[3]CONSTRUCT-GEO, Faculty of Engineering of Univ. of Porto, Rua Dr. Roberto Frias, s/n 4200-465 Porto, Portugal. E-mail: maxim.millen@gmail.com
[4]CONSTRUCT-GEO, Faculty of Engineering of Univ. of Porto, Rua Dr. Roberto Frias, s/n 4200-465 Porto, Portugal. E-mail: viana@fe.up.pt
[5]Dept. of Civil Engineering, Istanbul Univ., 34320 Avcilar, Istanbul, Turkey. E-mail: ssargin@istanbul.edu.tr
[6]Dept. of Civil Engineering, Istanbul Univ., 34320 Avcilar, Istanbul, Turkey, E-mail: sadikoztoprak@gmail.com
[7]Dept. of Civil Engineering, Istanbul Univ., 34320 Avcilar, Istanbul, Turkey. E-mail: kelesoglu@istanbul.edu.tr

ABSTRACT

This paper investigates the key parameters that influenced the settlement of a case study building on liquefiable soil in Adapazari (Turkey) during the 1999 Kocaeli earthquake. Ground movements in Adapazari caused large devastation, largely attributed to liquefaction of low plasticity silty soil layers underneath buildings on shallow foundations. The case study soil profile was well characterized by in-situ testing as well as laboratory tests from the Adapazari area. This allowed several different estimates of the building settlement to be obtained through different methods and through a variation in upper and lower bound estimates of the soil parameters. The different methods and different soil properties resulted in a wide range of estimates from 0.004 m to 1.6 m for the building settlement, compared to the observed in-situ value of 0.9 m. Even though the results were varied, the estimation of the liquefied strength of the soil appeared to be a key parameter for the settlement of the case study building. A detailed study with the PLAXIS finite-element software and UBC3D-PLM constitutive model, provided a consistent estimate of the final settlement of 0.9 m compared to the in-situ value. However, the limitation due to the enforced 'undrained' conditions during the dynamic phase of the analyses may have resulted in an inaccurate simulation of the pore water pressure and subsequently could have influenced the estimation of settlement. The modeling of the liquefaction settlements under free-field conditions was also considerably less than the re-consolidation settlements that were obtained through simplified procedures, suggesting that the re-consolidation settlement under the foundation was not modelled accurately. The present paper focuses on the assessment of the settlements due to earthquake-induced liquefaction as part of the research being conducted within the European project LIQUEFACT.

Keywords: Liquefaction; UBC3D-PLM; free field, soil-structure interaction, settlement, excess pore pressure

1 INTRODUCTION

On August 17, 1999, at 3:02 in the morning, a powerful earthquake struck through northern Turkey. This earthquake was later called the Kocaeli earthquake (after the name of the province where the epicentre was located) and was estimated as having a moment magnitude of 7.4. The Kocaeli earthquake generated intense interest within the engineering community due to reports of massive ground failures and structural collapse (Bay and Cox 2001). An investigation was made of the downtown area, in which damages were classified by its cause, i.e., inertia force or soil liquefaction. Hundreds of structures settled, slid, tilted, and collapsed due, in part, to liquefaction and ground softening (Bray et al 2011). Much of the devastation was attributed to the failure of the low plasticity non-plastic silts that had been deposited by the Sakarya River in its almost annual flooding of the plain over the past 7,000 years. It has recently been claimed that such fine-grained soils have a potential for liquefaction, similar to sands, a fact that was confirmed during the 1999 Marmara earthquake in Turkey (Arel and Önalp 2012).

The UBC3D-PLM is a constitutive model that provides a relatively simple but powerful approach to model the onset of the liquefaction phenomenon of sandy and non-plastic silty soils under the presence of an earthquake. The UBC3D-PLM is a 3-D generalized formulation of the original 2D UBCSAND model introduced by Puebla et al. (1997). This constitutive model has been implemented within PLAXIS (2017), a software based on the finite element method. The UBC3D-PLM model utilizes isotropic and simplified kinematic hardening rules for primary and secondary yield surfaces, in order to take into account the effect of soil densification and predict a smooth transition into the liquefied state during undrained cyclic loading (Petalas and Galavi 2013).

The goal of this paper is to assess the ability of UBC3D-PLM to reasonably simulate the post-liquefaction settlements under both free field conditions and under shallow foundation buildings. A case study of a building in Adapazari (Turkey) was numerically simulated using PLAXIS and the soil constitutive model UBC3D-PLM and the results were compared to in-situ observations and results from empirical analysis from CPTu results. To interpret this model several key physical parameters (e.g. soil friction angle, normalized penetration resistance of soil, ground motion intensity) were varied in order to study the influence of each one on the final settlement and excess pore pressure build up, as well as examining and varying key parameters in the constitutive model scheme.

2 CASE STUDY

The case study consisted of a simulation of a 4-story reinforced concrete building (named ‘Building F’ in Sancio (2003) and Bray and Macedo (2017)), in Figure 1, located along Sönmez Street, Yenigün District, Adapazari, Turkey during the Kocaeli earthquake of 1999. The GPS coordinates are N40.77148º and E30.40795º. This building has a length of 13 meters in the East-West direction and a major and minor width of 7.7 meters and 7.3 meters in the North-South direction. The height of the structure is 10.8 meters. Consistent with most of the foundation systems in the city of Adapazari, the foundation of this structure consists of a 0.40 meters thick reinforced concrete mat strengthened with 1.20 meters high tie beams (Sancio 2003).

According to field observations in 1999, 0.90 m of liquefaction-induced settlement was measured as the vertical distance between the top point of the heaved pavement and the bottom level of the foundation. Additionally, it translated approximately 0.25 meters towards the west and 0.30 meters to 0.40 meters to the north (Sancio 2003). Recently, Bray and Macedo (2017)

categorized the liquefaction-induced settlements of this building as shear and volumetric-induced which complies well with the observed displacements shown in Figure 1c. The building is still in use and the 45–50 cm residual settlement is still apparent (Figure 1d). Bray and Macedo (2017) indicate that shear induced settlements are primary displacements and are around 45 cm.

Two cone penetration tests (CPT), one seismic piezocone penetration test (SCPTU), one exploratory boring with standard penetration test (SPT) and considerable amount of laboratory tests including index properties, consolidation were performed in July, 2000 (after the earthquake), by Sancio (2003) to characterize the subsurface soil. Based on the q_c and f_r values given in **Figure 2**, the Adapazari silt between 1.5 - 5.5 meters is in a very loose state.

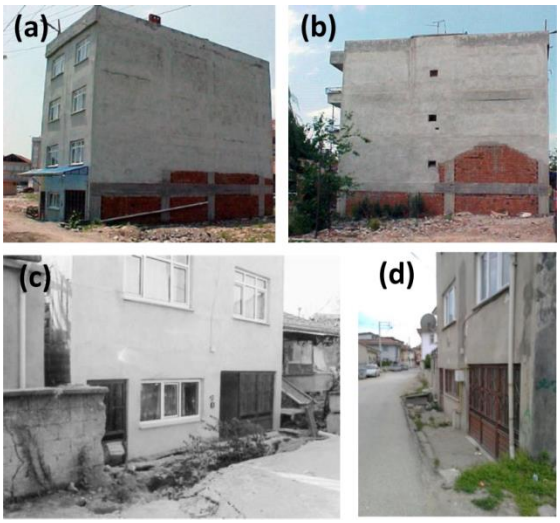

Figure 1. View of the F1 building; (a) from Sönmez street in 2000, b) from southeast side of site in 2000 (Sancio 2003), (c) just after earthquake on August 1999, (d) from Sönmez street in 2017

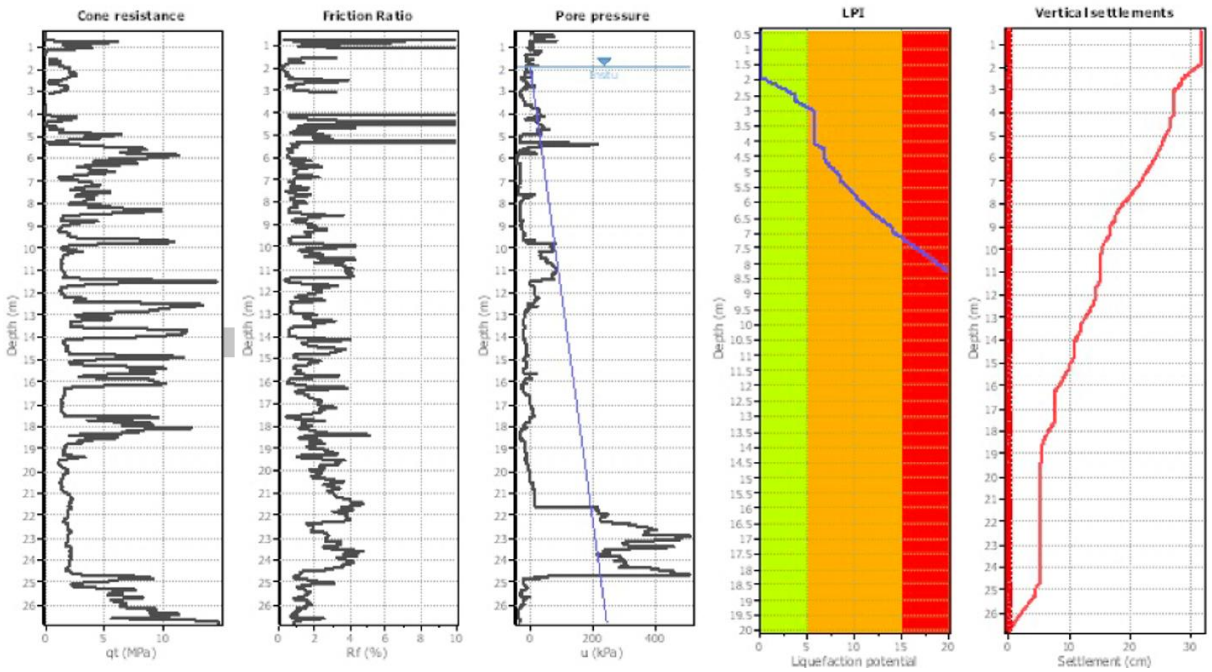

Figure 2. CLiq® analysis using the empirical methodologies

Table 1. Input parameters for simplified analysis

Property	Value
Height of crust [m]	2
Height of Liquefied layer [m]	8.5
Ground water level [m]	2
Crust friction angle [degrees]	31
Liquefied layer equiv. friction angle [degrees]	5.5
Foundation width [m]	7.6
Foundation depth [m]	1.0

3 ESTIMATION OF SETTLEMENTS

3.1 Free field conditions

The interpretation of CPT results was made using CLiq®, a software package specifically developed for liquefaction potential analysis. The vertical settlements in free-field conditions calculated by that software are based on the approach of Zhang et al. (2002) and Ku et al. (2012).

To perform the analysis, the ground motion was characterized by a magnitude of 7.2 and a PGA of 0.4 g according to Sancio (2003). These settlements were also analysed in PLAXIS as a free field case in the following sections. As presented in **Figure 2** a large portion of the profile is expected to liquefy and large surface settlement would be expected due to a high LPI (Liquefaction Potential index) (Iwasaki et al. 1982). The calculated settlement was 0.35 m.

3.2 With the structure

Liquefaction induced building settlement is a complex problem involving a vast range of structural, soil, foundation and hazard parameters. Many of these parameters provide a chaotic and almost contradictory influence on the settlement (e.g. increasing the foundation applied pressure can either increase or decrease settlements depending on the conditions). The estimation of the settlement therefore requires the accurate quantification of all of the influential variables, which is often difficult due to the cost of characterising the soil profile and difficulties with obtaining accurate measurements of the seismic demands. Even with accurate characterisation, there are still major shortcomings in many constitutive models used within finite-element software applications and the development of robust hand-calculation methods have been limited by the complexity of the problem. Regardless of these limitations, numerical, empirical and analytical approaches can provide a useful insight into the performance of a building on a liquefiable soil deposit.

Two simplified methods have been used in order to estimate the building settlement as an alternative to numerical estimation of the settlement performed in PLAXIS. The first method is a purely empirical approach using the relationships provided by Liu and Dobry (1997) from field investigations by Yoshimi and Tokimatsu (1977) and Adachi et al. (1992). The second is an analytical method by Karamitros et al. (2013), using a sliding block analogy and an estimate of the bearing capacity factor of safety of the liquefied deposit. The bearing capacity factor of safety was determined using slip plane analysis in the software LimitStateGeo (2017) where a two-layered soil profile was modeled using the properties summarised inTable **1**. The liquefied layer was modelled with a uniform degraded friction angle ($\phi_{degraded}$) of 5.5 degrees using the following equation, from Karamitros et al. (2013), where U is the average pore pressure in the zone of influence of the foundation:

$$\phi degrated = \tan^{-1}\left[\left(1-U\right)\tan\left(\phi_0\right)\right]$$

The settlement was calculated using the following equations from Karamitros et al. (2013):

$$Sett = c \cdot a_{\max} \cdot t_{cycle}^2 \cdot n_{cycles} \cdot \left(\frac{H_{liq}}{B}\right)^{1.5} \cdot \left(\frac{1}{FS}\right)^3$$

$$c = \min\left(0.003 \cdot \left(1.0 + 1.65 \cdot \frac{L}{B}\right), 0.035\right)$$

where the maximum cyclic acceleration, a_{max} = 0.4 m/s^2, the equivalent number of cycles, n_{cycles}=15 and the equivalent cyclic period, t_{cycles} = 0.35.

The bearing capacity was calculated as 10270 kN, providing a static factor of safety of 1.9 and a settlement of 0.015 m. The residual strength of liquefied soil is difficult to accurately estimate (Boulanger et al. 2013) and therefore the friction angle of the liquefied layer was varied in order to determine its influence. For degraded friction angles of 3.0 and 9.0, the bearing capacity factors of safety were 1.2 and 3.0 and the settlements were 0.054 m and 0.004 m, respectively. The sharp change in the bearing capacity factor of safety demonstrates the importance of accurately quantifying the liquefied strength for this case study. The crust depth was also varied in order to investigate the importance of the crust strength: crust depths of 1.5 m and 2.5 m caused settlements of 0.025 m and 0.009 m, respectively.

Since this building is close to static failure when the deposit liquefies (*FS*<1), the exact settlement is very sensitive to the magnitude of the strength parameters. The values from the Karamitros et al. (2013) method are shown in **Figure 3** along with the empirical values from Liu and Dobry (1997) and the measured value of 0.9 m (90 cm). The variation in the results is quite large, especially considering the value of 1.6 m obtained from the upper bound estimate from the curves from Liu and Dobry (1997).

4 NUMERICAL SIMULATIONS

In the present paper, the problem of liquefaction-induced building settlement is addressed from the numerical point of view as well. A reference benchmark model of the case study is constructed in PLAXIS and a parametric study is then developed to analyse the settlements and excess pore pressure occurring during and after an earthquake in scenarios where liquefaction can develop. This software has adequate features to deal with complex non-linear dynamic models. Some recent examples of the use of PLAXIS for liquefaction analysis are referred to Daftari and Kudla (2014) and Souliotis and Genolymos (2016), among others.

4.1 Numerical model

The considered soil profile (**Figure 4**) has three distinguishable layers. Sandy, silty and clayey layers with a total model thickness of 50 m overlying in a “C soil” depending on Eurocode 8 (Dense sand or gravel or stiff clay). The first liquefiable soil (layer 4) is Adapazari silt with a thickness of 3.2 m. Layer 5 is 3.4 m thick and composed of silty sand. Layer 7 is 4.0 m thick and composed of silty sand. The water table is located at a depth of 1.5 m. Layer 4, Layer 5 and Layer 7 were modelled with the UBC3D-PLM constitutive model as described in the next section. The depth of the model is 50 meters and the horizontal dimension is 200 meters to avoid wave reflections.

A four-story building is considered, with a total height of 10.8 meters and a width of 8

meters. The basement level is at 1.3 m depth measured from the ground floor.

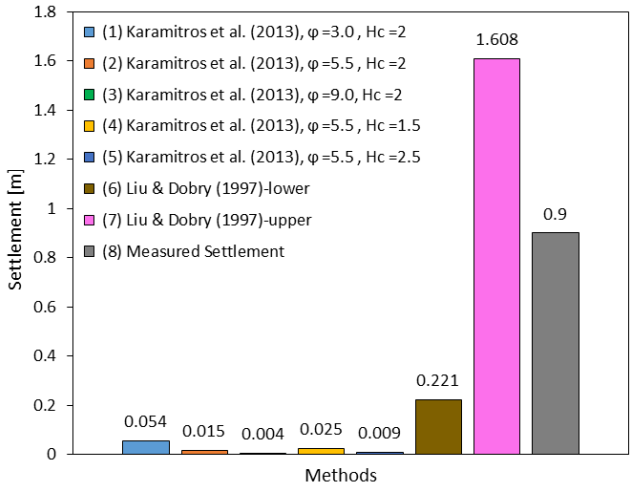

Figure 3 – Empirical and analytical estimates of settlement

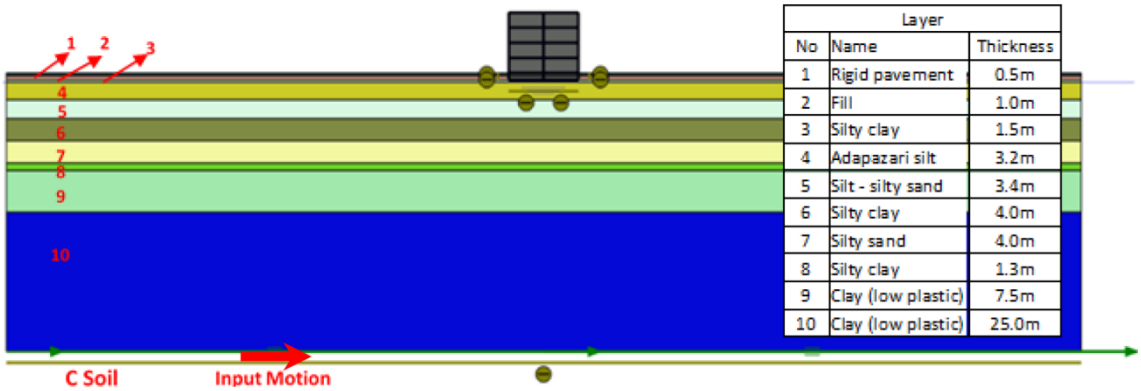

Layer		
No	Name	Thickness
1	Rigid pavement	0.5m
2	Fill	1.0m
3	Silty clay	1.5m
4	Adapazari silt	3.2m
5	Silt - silty sand	3.4m
6	Silty clay	4.0m
7	Silty sand	4.0m
8	Silty clay	1.3m
9	Clay (low plastic)	7.5m
10	Clay (low plastic)	25.0m

Figure 4 – Representation of the numerical model considered in the analyses

The finite element mesh was refined in the region closer to the embedded footing and gradually coarsened towards the left and right boundaries to provide a better discretization in the area of interest. Tied-degrees of freedom were adopted to simulate the infinite development of the domain along the horizontal direction during dynamic excitation, while a compliant base was selected at the base to allow soil overlying a bedrock to be able to absorb the downward propagating waves.

The outcrop data from the shaking event recorded in the EW direction in the south of the Adapazari city with a PGA of 0.4 g (4.07 m/s^2) was applied as an acceleration time history at the bottom of the model. **Figure 5** shows the input ground motion and **Figure 6** depicts the Vs profile deduced from Komazawa et al. (2002) and Ozcep et al. (2013). Relying on these references, the "C soil" was considered 50 meters below the ground surface (**Figure 6).**

4.2 Structure parameters

Structural elements are modelled assuming linear elastic behaviour and a representative rigidity. The walls and floors were modelled with beam elements. A weight of 10 kPa on each upper slab and 16 kPa on the foundation slab were assumed to simulate the structure weight of this case study. Interface elements with properties from the adjacent soil was applied between the

footing and the surrounding soil to account for the frictional interaction between the two.

4.3 Soil parameters

Two static phases, one dynamic phase and one consolidation phase were used to the simulations. For the static phases, the Hardening Soil with Small Strain constitutive model ("HS-Small model") was used (**Table 2**). This model has the capability of applying hysteretic damping dependent on the soil. The parameters for HS-Small model of each layer were determined by using the CLiq® and CPeT-IT®, a software package for the interpretation of Cone Penetration Test data based on the Robertson (2009) methodology. To obtain the unit weight, void ratio of soils and E_{oed} of interface were used consolidation tests results.

The UBC3D-PLM soil constitutive model was adopted to simulate the constitutive behaviour of the layers 4, 5 and 7 in the dynamic and consolidation phases. The HS-Small model was used for all other layers. UBC3D-PLM is a user-defined model implemented in PLAXIS, which can simulate seismic liquefaction behaviour of sands and silty clays. It is a non-linear, elasto-plastic, effective-stress-based model capable of capturing the evolution of excess pore pressures under undrained cyclic analysis. A detailed description about the constitutive model characteristics can be found in Petalas et al. (2012), and Galavi et al. (2013), among others. Most input parameters in the model have a physical meaning and can be derived from conventional laboratory tests or by empirical correlations with SPT values; while other parameters (e.g. me and ne) required curved fitting using laboratory data. **Table 3** gives the list of input parameters.

Since the UBC3D-PLM model depends primarily on $(N_1)_{60}$, q_c from Cone Penetration (CPT) tests was used to obtain $(N)_{60}$ as Robertson et al. (1986) suggested:

$$(N)_{60} = \frac{(q_c / p_1)}{I_c}$$

$$(N_1)_{60} = (N)_{60} \cdot C_N \cdot C_S \cdot C_R \cdot C_B$$

Here; p_a = Atmospheric pressure, Ic= Soil behaviour coefficient (1.5 for clays, 2.0 for silts, 3.0 for silty sands/sands) C_N = Geological stress correction, C_R = Rod length correction, C_S=Sampler tube Correction and C_B = Correction factor of borehole diameter.

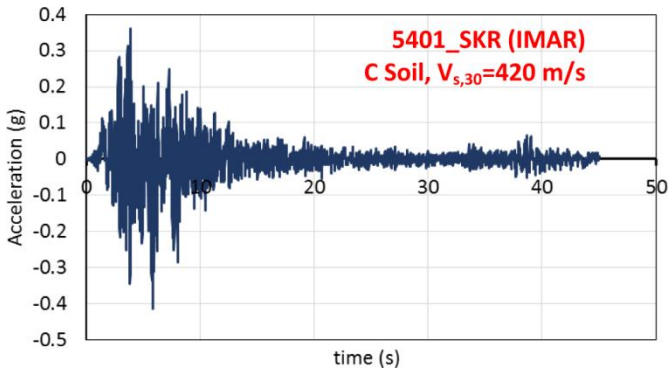

Figure 5. Input ground motion accelerogram named 5401_SKR (IMAR record)

The UBC3D-PLM model has been developed by Tsegaye (2010) and implemented as user-defined model in PLAXIS. It is closely based on the UBCSAND model introduced by Puebla et al. (1997), Beaty and Byrne (1998). Makra (2013) revised the proposed equations and highlighted the differences between the original UBCSAND formulation and the UBC3D-PLM as implemented in PLAXIS.

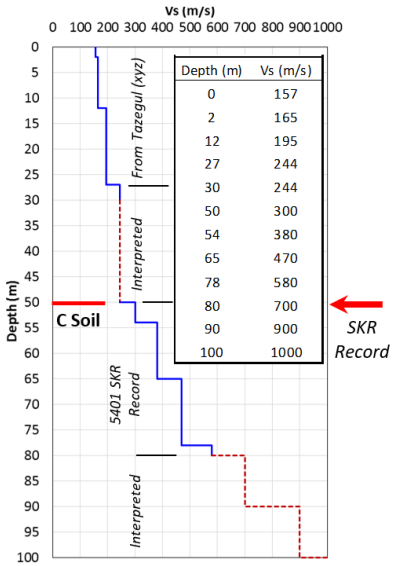

Figure 6. Considered Vs profile at Site F

The proposed equations for the generic initial calibration are as follows (Galavi et al. 2013):

$$K_G^e = 21.7 \cdot 20.0 \cdot (N_1)_{60}^{0.333}$$

$$K_B^e = K_G^e \cdot 0.7$$

$$K_G^p = K_G^e \cdot (N_1)_{60}^{2} \cdot 0.003 + 100.0$$

$$\varphi'_{pi} = \varphi'_{cv} + (N_1)_{60} / 10.0$$

where φ_{pi} is the peak friction angle for $(N_1)_{60}$ values lower than 15 while for larger an additional increase is suggested as described by the following relation:

$$\varphi'_p = \varphi'_{pi} + max\left(0.0, \frac{(N_1)_{60} - 15}{5}\right)$$

The values of me and ne are both considered equal to 0.5 and the value of np equal to 0.4 by default. For the failure ratio, Rf the following correlation applies:

$$R_f = 1.1 \cdot (N_1)_{60}^{-0.15}$$

5 NUMERICAL MODELLING RESULTS

The initial numerical model was setup using the parameters in **Table 2** and **Table 3** (best input parameters) in previous section. Using PLAXIS the liquefaction potential can be expressed by means of the excess pore pressure ratio (r_u), which represents the ratio of the excess pore pressure and the initial effective vertical stress at that depth. When the excess pore pressure ratio (r_u) is equal to 1.0 means complete liquefied state. Zones with excess pore pressure ratio (r_u) greater than 0.7 are considers in liquefied state (Beaty and Perlea 2011).

It is observed in **Figure 7** that almost the entire Adapazari silt (layer 4) reached liquefaction because of the high levels of excess pore pressures generated by the earthquake. No liquefaction occurs below 4.8 meters.

Shear-induced (Figure 8a) and volumetric-induced (Figure 8b) liquefaction settlements are approximately 90 cm (Figure 8c) as seen in **Figure** 1c and as explained in Bray and

Macedo (2017).

Table 2 – Input parameters for HS-Small model in PLAXIS

Parameter	Unit	Pavement (1)	Fill (2)	Silty Clay (3)	Adapazari Silt (4)	Silty Sand (5)	Silty Clay (6)	Silty Sand (7)	Silty Clay (8)	Clay (9)	Clay (10)
Unsaturated unit weight (γ_{unsat})	kN/m^3	20	16	16	16	16	17	16	16	17	18
Saturated unit weight (γ_{sat})	kN/m^3	21	17	17	17	17	18	17	17	18	19
Secant stiffness (E^{ref}_{50})	kN/m^2	100000	3111	4494	8211	18310	17950	24910	23120	31820	89470
Tangent stiffness oedometer load (E^{ref}_{oed})	kN/m^2	100000	2489	3595	6569	14650	14360	19930	18490	25450	71570
Unloading/reloading stiffness (E^{ref}_{ur})	kN/m^2	300000	9334	13480	24630	54930	53840	74730	69350	95450	268400
Power (m)	-	0.5	0.5	0.5	0.5	0.5	0.5	0.5	0.5	0.5	0.5
Initial void ratio (e_{init})	-	0.654	0.921	0.883	1.089	0.709	0.804	0.765	0.808	0.789	0.654
Cohesion at reference stress (c'_{ref})	kPa	10	1	1	1	1	1	1	1	1	1
Internal friction angle (φ')	(º)	36	30	30	30	31	30	30	30	30	31
Dilation angle (ψ)	(º)	5	0	0	0	1	0	0	0	0	1
Shear modulus (G_0)	kN/m^2	120000	32550	39840	49000	86200	85260	102100	97980	116800	206100
Shear strain at which Gs=0.722Go ($\gamma_{0.7}$)	-	0.003	0.003	0.003	0.003	0.003	0.003	0.003	0.003	0.003	0.003
Poisson's ratio for unload-reload (v_{ur})	-	0.3	0.3	0.3	0.3	0.3	0.3	0.3	0.3	0.3	0.3

In order to assess the influence of key parameters on the ability of the UBC3D-PLM constitutive model to simulate the liquefaction cases with the presence of the structure, several parameters were systematically varied (**Table 4**).

Figure 9 presents the vertical displacement at the bottom of the structure for the cases defined in **Table 4** and **Figure 10** the excess pore pressure build up at a depth of 4.7 m.

The first comparative analysis is Case 1, where the SPT value was changed from 3.0 as 5.0 (**Table 4**), in order to reflect the upper bound value measured in the field investigations. Also, a lower value of $(N_1)_{60}$ was adopted in order to reflect a silty sand (Case 2). In the analysis presented as Case 3, the GWL was modified from 1.5 m to 2.1 m to reflect potential seasonal variations.

Table 3 - Input parameters of the UBC3D-PLM model in PLAXIS

	Parameter	Unit	Adapazari Silt (4) [Bench-mark]	Silt-Silty Sand (5)	Silty Sand (7)	Adapazari Silt (4) [lower]	Adapazari Silt (4) [upper]
UBC Sand Input Parameters	Constant volume friction angle (φ_{cv})	(º)	30	30	30	30	30
	Peak friction angle (φ_p)	(º)	31	31	30	30.4	31.6
	Cohesion (c)	kPa	-	-	-	-	-
	Elastic shear modulus (K^e_G)	-	872.1	1162	1049	688.7	945
	Elastic plastic modulus (K^p_G)	-	123.5	448.5	301.4	108.3	125.5
	Elastic bulk modulus (K^e_B)	-	610.5	213.3	734.3	482.1	661.5
	Elastic shear modulus index (ne)	-	0.5	0.5	0.5	0.5	0.5
	Elastic bulk modulus index (me)	-	0.5	0.5	0.5	0.5	0.5
	Plastic shear modulus index (np)	-	0.4	0.4	0.4	0.4	0.4
	Failure ratio (R_f)	-	0.933	0.779	0.805	0.991	0.864
	Atmospheric pressure (PA)	kPa	100	100	100	100	100
	Tension cut-off (σ_t)	kPa	0	0	0	0	0
	Densification factor (fac_{hard})	-	1	1	1	1	1
	SPT value $(N_1)_{60}$	-	3	10	8	2	5
	Posliquefaction factor (fac_{post})	-	1	1	1	1	1
Interface properties	Oedometer modulus of soil (E^{ref}_{oed})	kPa	6569	44830	53090	6569	6569
	Cohesion at references stress (c'_{ref})	kPa	1	1	1	1	1
	Internal friction angle (φ')	(º)	30	31	30	30	30
	Dilation angle (ψ)	(º)	0	1	0	0	0

As shown in **Figure 9**, $(N_1)_{60}$ has a considerable effect on shear and volumetric induced settlements, as it significant alters the liquefaction potential of the soil as seen in the change in the build-up of pore pressure in **Figure 10**. On the other hand, water level did not have a very significant influence on the final settlement. The results are in line with the simplified procedure from Karamitros et al. (2013) (Section 3.2) where the settlement was very sensitive to the estimation of the liquefied soil strength. In all of the simulated cases, the majority of the settlement occurred during the shaking, the only simulation that showed a significant increase in settlement after shaking was the upper bound $(N_1)_{60}$. The upper bound $(N_1)_{60}$ case also showed an increase in pore pressure after shaking, suggesting that the bearing capacity would be further reduced and static shear-induced settlement would occur.

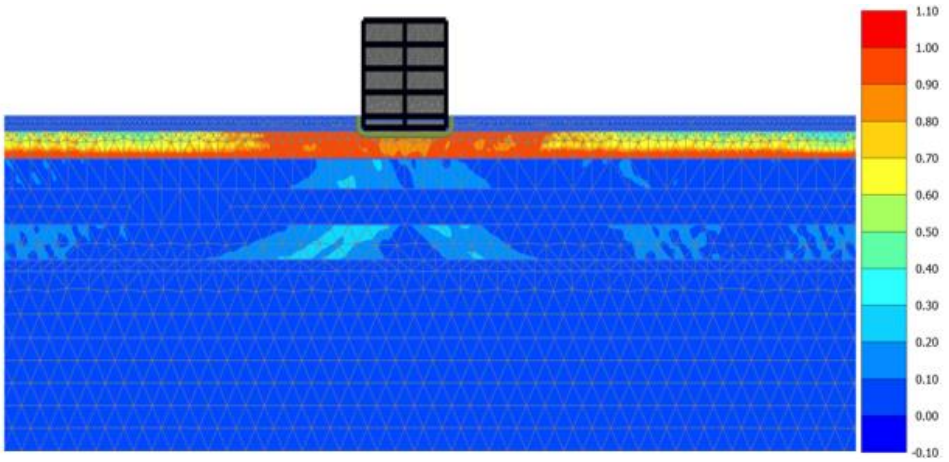

Figure 7. r_u values with structure presence (with best input parameters)

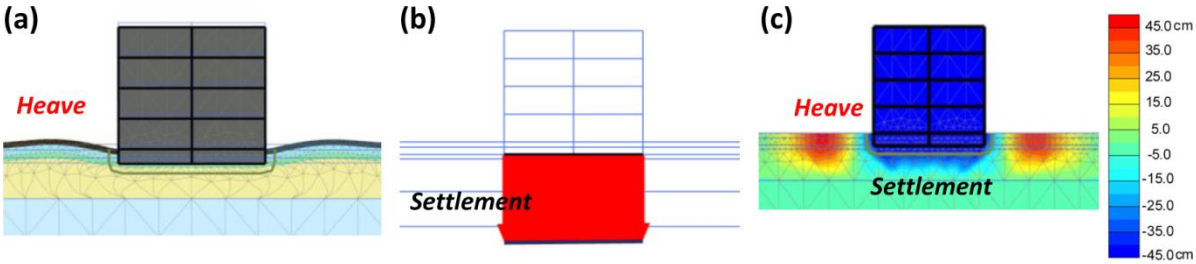

Figure 8. Obtained displacement patterns in PLAXIS; (a) Shear-induced, (b) Volumetric-induced, (c) Total settlements

Table 4. Results of the analyses with the presence of the structure

Case	Name	Variation	Liquefaction-induced Settlement [cm]
0	Best input	Layer 4: $(N_1)_{60}$=3, GWL= 1.5m	87.4
1	Upper $(N_1)_{60}$	Layer 4: $(N_1)_{60}$=5	13.7
2	Lower $(N_1)_{60}$	Layer 4: $(N_1)_{60}$=2	112.3
3	Lower GWL	Layer 4: $(N_1)_{60}$=3, GWL = 2.1m	80.1

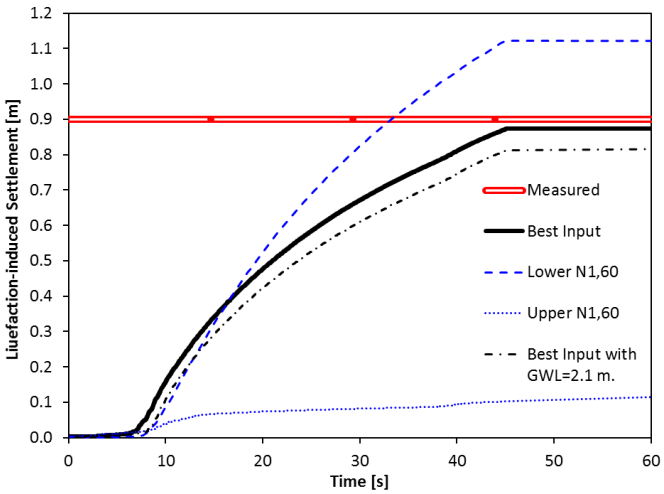

Figure 9. Results of settlements obtained with software PLAXIS for different parameters

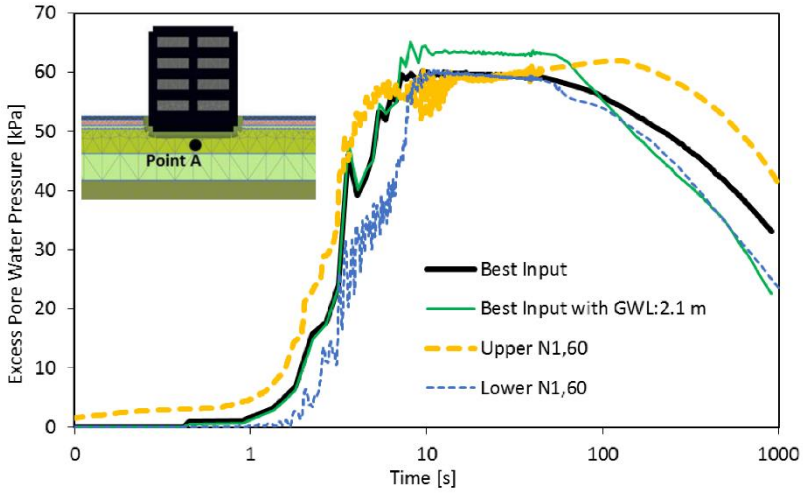

Figure 10. Excess pore pressure build-up obtained in PLAXIS for different parameters

Lower ground water level (Case 3) changed the dissipation of pore pressure during shaking, but did not reflect a significant change in the settlement during shaking or the post-shaking settlement. The issues related to post-shaking settlement are investigated further in the next section.

Several interesting aspects of the pore pressure build-up can be noted from **Figure 10**. The initial outcome is rapid mobilisation of excess pore pressures within ten seconds, which is expected, since the soil is in a relatively loose state. The excess pore pressure reaches a stable state at approximately 10 seconds, cycling at excess pore pressure of approximately 60 kPa, slightly higher than the free-field maximum excess pore pressure of 50 kPa, the high pore pressure is due to the additional stress from the building. The pore pressure then dissipates when shaking ends (after 50 seconds). The stable high excess pore pressure under the building reflects a limitation of the PLAXIS software, in that the dynamic action is modeled with 'un-drained' conditions, therefore pore water flow is not modelled during shaking. It could be expected that during shaking, some pore water would flow to or from the free-field and dissipation could happen during shaking.

5.1 Free field conditions

A simple numerical simulation of the case study without the presence of the building was set up to examine the UBC3D-PLM model. The model was setup using parameters in **Table 2** and **Table 3**. From **Figure 11**, it can be seen that almost the whole of Layer 4 reaches liquefaction, however, no liquefaction occurs at a depth of 4.8 to 50 meters.

The results of settlement and the development of excess pore pressure build-up at a depth of 4.7 m are presented in **Figure 12** and **Figure 13**, respectively. The calculated settlement in PLAXIS was approximately 0.02 meters. This value is very different from the estimated settlement from CLiq (0.35 m) and reflects the difficulty of modelling the re-consolidation and sedimentation process using this constitutive model. The resulting post-shaking building settlements from the previous section may therefore be underestimated if re-consolidation settlements are expected to be significant.

The expected pore pressure build-up is consistent with the CLiq factor of safety calculations as observed in **Figure 2** where the Layer 4 is completely liquefied below the ground water level.

It can also be seen in **Figure 13** that liquefaction occurs within a few seconds of the beginning of shaking. It is important to emphasize that the numerical simulations presented in this paper are performed using undrained effective stress conditions.

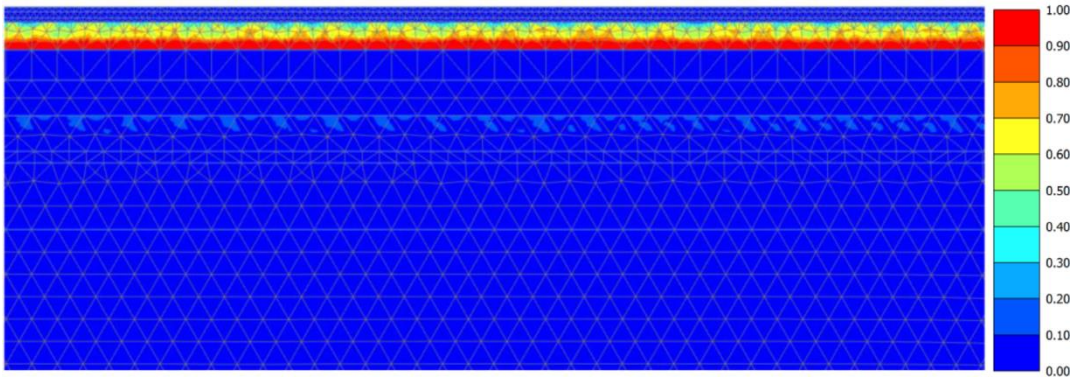

Figure 11. Excess pore water pressure ratio values (r_u) in free field conditions (after the earthquake)

Most settlements occur in the after shaking reconsolidation phase and the settlement during the earthquake shaking is insignificant. Because of the zero change in volume assumption of undrained analyses, the program was only able to accumulate the values of excess pore pressure ratios (r_u) until the end of the shaking motion with negligible vertical deformations arising from the ground motion.

CONCLUSIONS

The goal of this paper was to understand the key aspects that influenced the settlement of a case study building on liquefiable soil in Adapazari (Turkey) during the 1999 Kocaeli earthquake. The investigation involved the dynamic effective stress analysis of the case study building using UBC3D-PLM model implemented in the PLAXIS software, as well as an assessment of the bearing capacity using the LimitStateGeo software and the calculation of the liquefaction triggering and free-field settlement using the method of Zhang et al. (2002) in the CLiq software. The empirical chart from Liu and Dobry (1997) and the simplified analytical method from Karamitros et al. (2013) were also used to provide estimates of building settlement. The numerical, empirical and analytical estimates were compared with the in-situ observations of the building settlement.

Several parameters were varied in the numerical and analytical analyses to understand their influence on the expected level of settlement. The analytical analyses of the bearing capacity highlighted that the foundation was close to bearing capacity failure at the liquefied state, with factors of safety varying from 1.2 to 3.0 and was strongly influenced by the expected liquefied strength of the soil. The analytical settlement estimates (upper-bound: 0.05m) were all lower than the observed in-situ value of 0.9m, while the empirical values taken from the lower and upper lines on the chart from Liu and Dobry (1997) were 0.2m and 1.6m respectively.

The benchmark numerical settlement of 0.9 m was consistent with the observed in-situ value. The settlement of the PLAXIS model was also very sensitive to the variation of $(N_1)_{60}$ during the dynamic action, which altered the build-up of pore pressure and the effective strength of the liquefying soil. Further investigation into the pore pressure build-up highlighted some potential inaccuracies due to the inability to model pore water flow during the dynamic analysis because

conditions were modeled as undrained. A higher excess pore water pressure under the foundation compared to the free-field was observed in the analyses which in reality may have resulted in pore pressures dissipating during shaking instead of remaining stable throughout the later part of the shaking. The strong influence of soil strength from the simplified analytical analyses, suggests that the dynamic settlement may be influenced by this limitation.

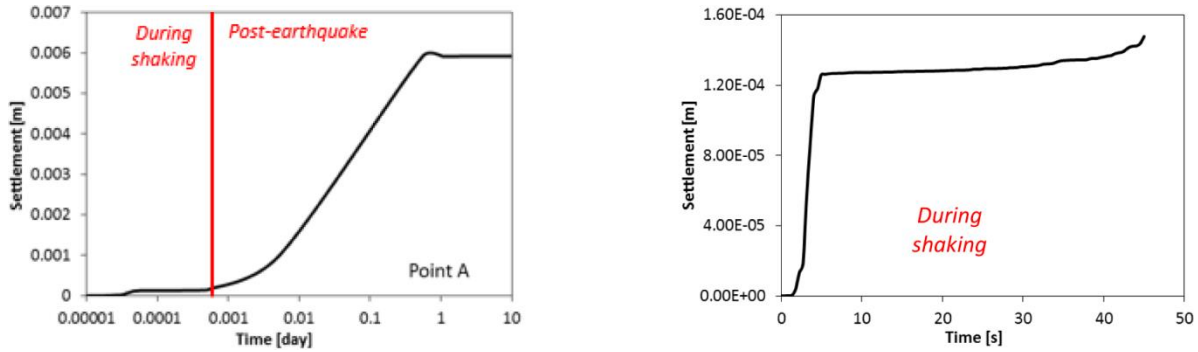

Figure 12. Final settlement using PLAXIS analysis in free field conditions

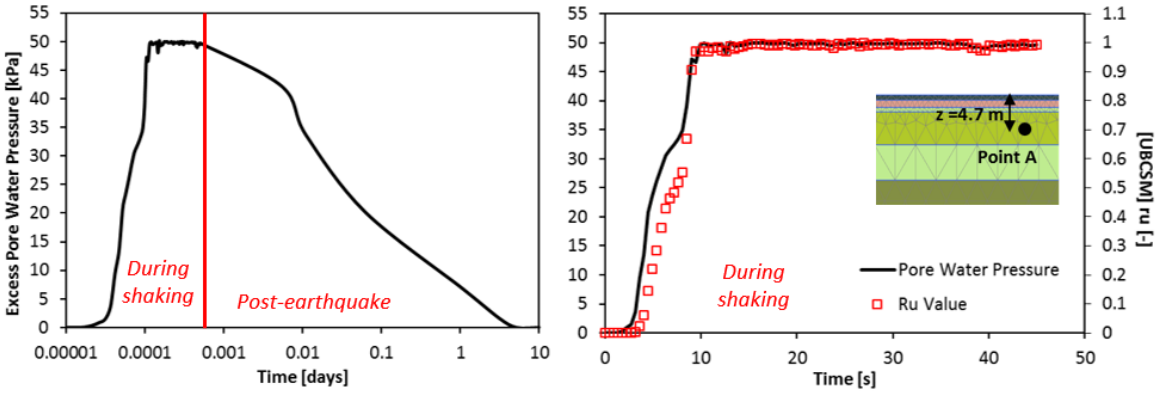

Figure 13. Development of pore pressure using PLAXIS analysis in free field conditions

Another observed limitation was the low estimate of the post-liquefaction reconsolidation settlement from the UBC3D-PLM constitutive model. A 'free-field' numerical simulation was conducted of the case study site without the presence of the building and the settlement that was obtained was only 0.02 m, which was considerably different to the value of 0.35 m obtained through the simplified method by Zhang et al. (2002). This may indicate that the post-liquefaction settlements from the numerical simulations were underestimated.

This multi-part study resulted in a considerable variation in the estimation of settlement between the methods employed, however, the strength of the liquefying soil appeared to be a key parameter in the settlement of the case study building. Improvements to future estimates of building settlements could benefit by better characterising the soil strength. The two limitations that were recognised in the numerical simulations of this case study (inability to capture pore water flow during shaking and re-consolidation settlement), may or may not be significant for other soil-foundation-building systems depending on the geometry, dynamics and other properties of the system. However, the user of any numerical tool should understand the limitations of their models. In relation to the success of PLAXIS for obtaining shear induced displacements it may lead to further understanding of the effects that influence building settlement in complex environments, such as in the presence of adjacent buildings.

ACKNOWLEDGEMENTS

LIQUEFACT project ("Assessment and mitigation of liquefaction potential across Europe: a holistic approach to protect structures / infrastructures for improved resilience to earthquake-induced liquefaction disasters") has received funding from the European Union's Horizon 2020 research and innovation programme under grant agreement No GAP-700748

REFERENCES

Adachi, T., Iwai, S., Yasui, M. and Sato, Y. (1992). "Settlement and inclination of reinforced concrete buildings in Dagupan City due to liquefaction during the 1990 Philippine earthquake". *Earthquake Engineering, Tenth World Conference*. Pp. 147–152.

Arel, E. and Önalp, A. (2012). "Geotechnical properties of Adapazari silt". *Bulletin of Engineering Geology and the Environment*, 71(4): 709–720.

Bay, J. A. and Cox, B. R. (2001). "Shear wave velocity profiling and liquefaction assessment of sites shaken by the 1999 Kocaeli, Turkey earthquake." *PEER Project Report SA3017-18336*, Pacific Earthquake Engineering Research, Berkeley, CA.

Beaty, M. and Byrne, P. (1998). "An effective stress model for predicting liquefaction behaviour of sand", *Geo. Earthquake Engineering and Soil Dynamics*., 1:766–777.

Beaty, M. H. and Perlea, V. G. (2011). "Several observations on advanced analyses with liquefiable materials". *Thirty first annual USSD conference on 21st century dam design-advances and adaptations*, 1369–1397.

Boulanger, R. W., Kamai, R. and Ziotopoulou, K. (2013). "Liquefaction induced strength loss and deformation: simulation and design". *Bulletin of Earthquake Engineering*, 12(3):1107–1128.

Bray, J. D. and Macedo, J. (2017). "6th Ishihara lecture: Simplified procedure for estimating liquefaction induced building settlement". *Soil dyn earthq eng*, 102: 215–231.

Bray, J. D., Sancio, R. B., Durgunoglu, T., Onalp, A., Youd, T. L., Stewart, J. P., Seed, R. B., Cetin, O. K., Bol, E., Baturay, M. B., Christensen, C. and Karadayilar, T. (2011). "Subsurface characterization at ground failure sites in Adapazari, Turkey". *J. Geotech. Geoenviron. Eng.*, 130(7): 673–685.

Daftari, A. and Kudla, W. (2014). "Prediction of soil liquefaction by using UBC3D-PLM model in Plaxis". *International Scholarly and Scientific Research and Innovation*. 8(2):106–111.

Galavi, V., Petalas, A. and Brinkgreve, R. (2013). "Finite element modelling of seismic liquefaction in soils". *Geotechnical Engineering Journal of the SEAGS & AGSSEA*, 44(3), 44(3): 55–64.

Iwasaki, T., Arakawa, T., Tokida, K. (1982). "Simplified Procedures for Assessing Soil Liquefaction During Earthquakes". *Proceedings of Conference on Soil dyn earthq eng.* Southampton; 1982, pp. 925–39.

Karamitros, D. K., Bouckovalas, G. D. and Chaloulos, Y. K. (2013). "Seismic settlements of shallow foundations on liquefiable soil with a clay crust". *Soil dyn earthq eng, 46*, 64–76.

Komazawa, M., Morikawa, H., Nakamura, K., Akamatsu, J., Nishimura, K., Sawada, S., Erken, A. and Onalp, A. (2002). "Bedrock structure in Adapazari, Turkey—a possible cause of severe damage by the 1999 Kociaeli earthquake". *Soil dyn earthq eng*, 22: 829–836.

Ku, C. S., Juang, C. H., Chang, C. W. and Ching, J. (2012). "Probabilistic version of the Robertson and Wride method for liquefaction evaluation: Development and application". *Can. Geotech. J*, 49(1): 27–44.

LimitStateGeo. (2017). "LimitStateGeo. LimitState". http://www.limitstate.com/geo
Liu, L. and Dobry, R. (1997). "Seismic Response of Shallow Foundation on Liquefiable Sand". *J. Geotech. Geoenviron. Eng.,* 123(6):557–567.
Makra, A. (2013). "Evaluation of the UBC3D-PLM constitutive model for prediction of earthquake induced liquefaction on embankment dams", *MSc Thesis*, TU Delft.
Ozcep, T., Ozcep, F. and Ozel, O. (2013). "V_S30, site amplifications and some comparisons: The Adapazari (Turkey) case". *Physics and Chemistry of the Earth*, 63: 92–101.
Petalas, A., Galavi, V. and Brinkgreve, R. (2012). "Validation and verification of a practical constitutive model for predicting liquefaction in sands". *Proceedings of the 22nd European young geotechnical engineers conference*, 167–172.
Petalas, A. and Galavi, V. (2013). "PLAXIS liquefaction model UBC3D-PLM". *PLAXIS.*
PLAXIS (2017). Information available on *https://www.plaxis.com/*
Puebla, H., Byrne, P. M. and Phillips, R. (1997). "Analysis of CANLEX liquefaction embankments: prototype and centrifuge models". *Can. Geotech. J*, 34:641-657.
Robertson, P. K., Campanella, R. G., Gillespie, D. and Greig, J. (1986). "Use of Piezometer Cone data". *In-Situ'86 Use of In-situ testing in Geotechnical Engineering*, pp 1263–1280.
Robertson, P. K. (2009). "Interpretation of Cone Penetration Tests – a unified approach". *Can. Geotech. J*. 27(1): 151–158.
Sancio, R. B. (2003). "Ground failure and building performance in Adapazari, Turkey". *PhD Thesis, University of California*, Berkeley.
Souliotis, C. and Gerolymos, N. (2016). "Seismic effective stress analysis of quay wall in liquefiable soil: the case history of Kobe". *International journal of Geomate*, 10 (2): 1770-1775.
Tsegaye, A. (2010). "Plaxis liquefaction model", external report.
Yoshimi, Y. and Tokimatsu, K. (1977). "Settlement of buildings on saturated sand during earthquakes". *Soils and Foundations*, 17(1):23–28.
Zhang, G., Robertson, P. K. and Brachman, R. (2002). "Estimating liquefaction-induced ground settlements from CPT for level ground". *Can. Geotech. J*, 39:1168-1180.